



A Drug-Free Tumor Therapy Strategy: Cancer-Cell-Targeting Calcification

Ruibo Zhao, Ben Wang, Xinyan Yang, Yun Xiao, Xiaoyu Wang, Changyu Shao, and Ruikang Tang*

Abstract: Herein, we propose a drug-free approach to cancer therapy that involves cancer cell targeting calcification (CCTC). Several types of cancer cells, such as HeLa cells, characterized by folate receptor (FR) overexpression, can selectively adsorb folate (FA) molecules and then concentrate Ca^{2+} locally to induce specific cell calcification. The resultant calcium mineral encapsulates the cancer cells, inducing their death, and in vivo assessments confirm that CCTC treatment can efficiently inhibit tumor growth and metastasis without damaging normal cells compared with conventional chemotherapy. Accordingly, CCTC remarkably improve the survival rate of tumor mice. Notably, both FA and calcium ions are essential ingredients in human metabolism, which means that CCTC is a successful drug-free method for tumor therapy. This achievement may further represent an alternative cancer therapy characterized by selective calcification-based substitution of sclerosis for tumor disease.

Cancer is a major cause of mortality worldwide, and its incidence continues to increase, with more than 10 million new cases every year.^[1] Currently, the conventional treatments for cancers are limited to chemotherapy, radiotherapy, and surgery. Unfortunately, chemotherapy and radiotherapy often have negative effects on normal cells, resulting in serious side effects, such as neuropathy, neutropenia, and kidney failure.^[2] Although surgery may completely remove primary tumors and visible metastases, the propensity of tumors to invade adjacent tissues or spread to distant sites by

micrometastasis often limits its effectiveness.^[3] Recent rapid advances in nanotechnology have contributed greatly to achievements in cancer treatment, however, both the in vivo cytotoxicity and the biosecurity of nanoparticles have been sources of controversy, especially the unexpected accumulation of nanomaterials in the body, which has been investigated in biomedical applications.^[4]

In nature, mineral accumulations are important biological processes. Calcification, as well as the accumulation of calcium salts in body tissues, normally occurs during the formation of bone and teeth.^[5] However, calcium can also be deposited abnormally in soft tissues, inducing pathological diseases, such as vascular calcification, skin necrosis, and kidney stones.^[6] Biological calcifications can be precisely regulated with solution medium balances or mineral nucleation sites. In 2008, we demonstrated bio-inspired cell encapsulation using controlled cell calcification, which followed an attractive hypothesis that cancer cells can be inhibited using calcification-based cell capsulation.^[7] Encapsulating the single-cell-organism with a thin functional coat can alter its behavior,^[8] however, even in vitro covering mammalian cells with a thin mineral layer is not biocompatible.^[9] Thus, targeting calcification on tumor cells without damaging normal cells is a great challenge.

It is well known that folate receptors (FR) are up-regulated in many human carcinomas but are expressed at low levels in normal cells,^[10a] and FR can specifically bind to and cause the accumulation of folic acid (FA) molecules. The established understanding of calcification indicates that FA may actively induce calcification owing to its carboxylate residues, which can specifically bind Ca^{2+} from biological fluids to facilitate calcium mineral nucleation.^[10] Thus, it is reasonable to expect that abundant FRs on cancer cells can be used to develop cancer cell targeted calcification (CCTC; Supporting Information, Figure S1) using adsorbed FA biomolecules.

In this study, we demonstrated CCTC using human embryonic kidney (HEK293) and human cervical cancer (HeLa) cell lines, which were selected as models of FR-deficient normal cells and FR-rich cancer cells, respectively. In vivo experiments show that CCTC can inhibit tumor growth and their secondary metastases. It should be noted that both calcium and FA are essential ingredients in human metabolism.^[11] Therefore, CCTC represents a drug-free strategy for cancer treatment.

In vitro CCTC was seen after incubating cells with Dulbecco's Modified Eagle Medium (DMEM) containing $500 \mu\text{g mL}^{-1}$ FA, followed by the addition of DMEM containing 10 mM Ca^{2+} . Both native HEK293 and HeLa cells

[*] R. Zhao, C. Shao, Prof. Dr. R. Tang
Center for Biomaterials and Biopathways
Department of Chemistry, Zhejiang University
Hangzhou, Zhejiang 310027 (China)
E-mail: rtang@zju.edu.cn

B. Wang, Y. Xiao
Cancer Institute, The Second Affiliated Hospital of
Zhejiang University College of Medicine
Hangzhou, Zhejiang 310009 (China)
and
Institute of Translational Medicine
Zhejiang University College of Medicine
Hangzhou, Zhejiang 310029 (China)

X. Yang
Institute of Biological Engineering
Zhejiang Academy of Medical Sciences
Hangzhou, Zhejiang 310013 (China)

X. Wang, Prof. Dr. R. Tang
Qiushi Academy for Advanced Studies, Zhejiang University
Hangzhou, Zhejiang 310027 (China)

Supporting information for this article can be found under:
<http://dx.doi.org/10.1002/anie.201601364>.

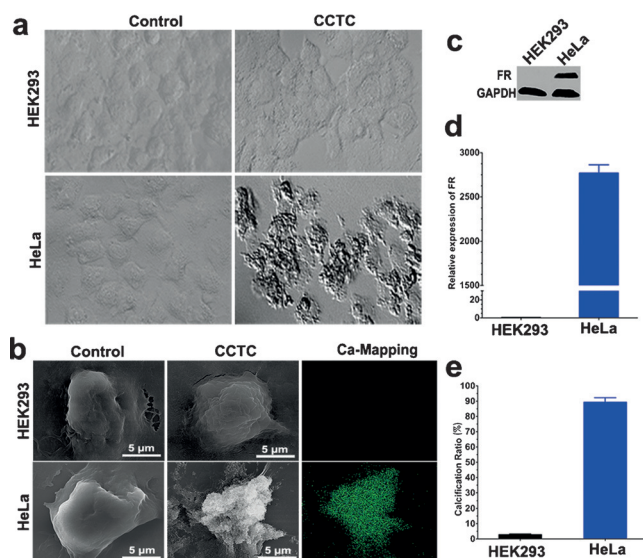


Figure 1. Selective CCTC mediated by FA. Optical (a) and scanning electron microscopy (b) observations of HEK293 and HeLa cells. Relative expression of FR in HEK293 and HeLa cells by western blot (c) and qPCR (d). e) Calcification ratio of HEK293 and HeLa cells.

showed representative adherent cellular morphology (Figure 1a, Control) with smooth surfaces before CCTC (Figure 1b). After CCTC, the smooth surfaces of the HEK293 cells were maintained, and no calcium deposition was noted. However, calcification occurred in the HeLa cells, resulting in the formation of a rough solid layer around the cells (Figure 1a and 1b), which consisted of numerous tiny particles (Figure S2a). X-ray diffraction, FTIR, and calcium element mapping analyses confirmed that the calcified mineral around the cancer cells was amorphous calcium phosphate (Figure S2b and S2c). Compared with the HEK293 cells, which had almost no FR expression and insignificant calcification ($< 3\%$), the HeLa cells presented a notable calcification rate ($> 90\%$) owing to high FR overexpression, which suggested the occurrence of highly specific calcification in FR-overexpressed cancer cells (Figure 1c–e). It should be noted that any individual treatment using either FA or Ca alone resulted in no calcification (Figure S2d and S2e). Therefore, the key to CCTC was the combination of FA and calcium, which induced calcification. More cells with different FR levels were examined, and the results suggested a moderately positive correlation between cell calcification and FR expression (Figure S3).

The resultant mineral phase may affect cell viability, especially because mammalian cell membranes are extremely sensitive to any adherent foreign solid matter.^[9,12] Viewed with confocal laser scanning microscopy (CLSM), the deposited CaP layer (green, labeled by Calcein) attached tightly to the cell membrane (red, labeled by PKH26), resulting in a shell-like structure (Figure 2a). Owing to the presence of CaP matter, the integrity of the cell membrane was disrupted, resulting in fracture from 0 h to 24 h (Figure 2a). Meanwhile, nuclear (blue, labeled by Hoechst33342) shrinkage in the encapsulated cell could be detected (Figure 2a). This phenomenon indicated damage to the cell membrane structure

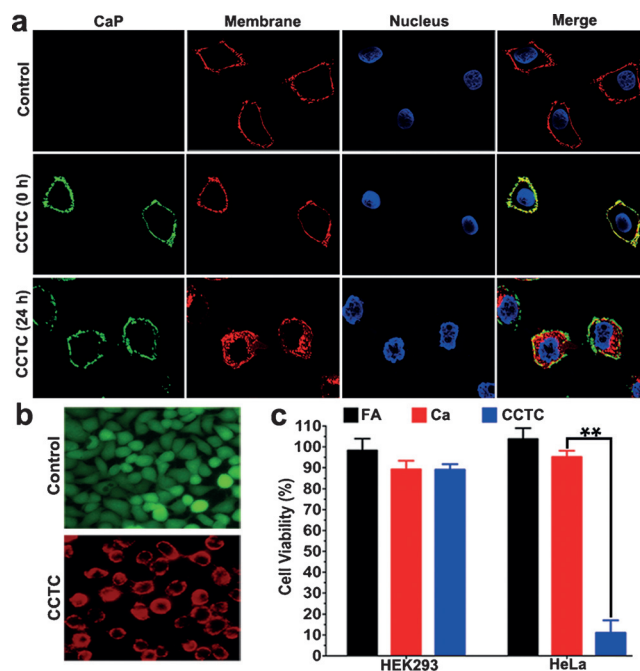


Figure 2. Cell viability after CCTC treatment. a) Fluorescent detection of calcified HeLa cells by confocal laser scanning microscopy (CLSM). CaP was stained by Calcein (green), the cell membrane was stained by PKH26 (red), and the nucleus was stained by Hoechst33342 (blue). b) Live/Dead staining suggested that the CCTC-treated HeLa cells were dead at 24 h. c) Quantitative analysis of cell viability with different treatments (** $P < 0.01$).

and cell death. The changes to both the membrane and the nucleus demonstrated that cell viability was reduced following calcification. Using LIVE/DEAD probes (Figure 2b), it was confirmed that almost all of the calcified HeLa cells were dead within 24 h; however, the native cells remained alive. Cells experienced calcification-encapsulation-induced cell death; fortunately, this effect occurred in cancer cells rather than in normal cells. MTT (3-(4,5-dimethylthiazol-2-yl)-2,5-diphenyltetrazolium bromide) assays were also conducted to quantitatively examine the anticancer effects of CCTC. The results indicated effective cancer cell growth inhibition ($> 90\%$), and in contrast, the influence of CCTC on HEK293 cells resulted only in negligible cell growth inhibition ($< 10\%$; Figure 2c).

Based on ectopic calcification in several pathological diseases,^[13] CCTC may be able to convert cancer tissues into “pathologically calcified” tissues through an encapsulation effect. To test this hypothesis, mice bearing HeLa xenografts were used to examine CCTC at the tissue level. The xenografts in the controls exhibited common solid tumor features, whereas the color of the tumors subjected to CCTC treatment turned yellow (Figure 3a). The tumors were subjected to micro-computed tomography (μ CT). If any calcified matter formed within a tumor, μ CT scanning would reveal its presence owing to the high density of the mineral phase.^[14] Tumor tissue was maintained in a homogeneous state without foreign matter in the control group (Figure 3b, Control). In contrast, a large amount of calcified matter could be detected within tumor tissues after CCTC

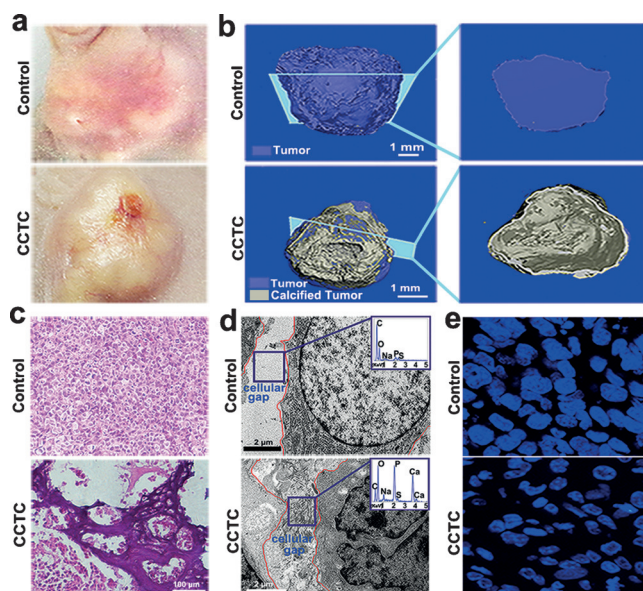


Figure 3. In vivo CCTC treatment effects on tumors. a) Optical images of calcified tumors; the tumor tissue became disrupted after CCTC treatment. b) μ CT detection of the tumors. The left column shows a three-dimensional reconstruction, and the right was a typical tomography section marked on the left. c) H&E staining of a tumor section. d) TEM observation and EDX (inset) of calcified matter in tumor cellular gaps. e) CLSM images of a tumor slice stained by Hoechst33342.

treatment (Figure 3b, CCTC), and hematoxylin and eosin (H&E) staining of tumor slices showed dark purple regions (Figure 3c), which was similar to the appearance of ectopic calcification.^[15] Furthermore, calcified matter was identified in cellular gaps by transmission electron microscopy (TEM), and energy dispersive X-ray (EDX) analysis confirmed that this material was CaP (Figure 3d). However, no CaP was noted in the tumor tissues subjected to FA or Ca treatment alone, nor was CaP noted in the control group; their cellular gaps remained clear (Figure 3d). This in vivo tissue-level result was in agreement with the cell-level in vitro results following sclerosis of tumor tissue by CCTC.

The CaP material formed by ectopic calcification could ulcerate calcific lesions and facilitate cell dysfunction and death,^[16] which was also observed in the CCTC treatment group (Figure 3a). In the control experiment, the cell nuclei in the tumor tissue showed normal morphology, whereas the nuclei became agglutinate and abnormal in the CCTC group (Figure 3e), indicating that the calcified state of the tumor tissue could intrinsically lead to cancer cell death. Furthermore, it should be noted that no calcification or tumor ulceration was detected after individual FA or Ca treatment (Figure S4), and hematological and blood biochemistry parameters, as well as the H&E staining results of the major organs, showed no pathological changes compared with the controls (Figure S5). These results implied that no damage to other tissues or organs was caused by CCTC in vivo.^[17]

Given the successful targeting calcification in tumor tissues, mice bearing HeLa tumor were treated by CCTC to investigate its anticancer effects. As shown in Figure 4a, DOX formulation, as a positive control, had a significant tumor

growth inhibition (TGI, 67.1 %) with respect to the inhibition of tumor growth compared with the control. Meanwhile, CCTC treatment showed similar anticancer effects with a TGI value of 65.1 %, and H&E staining showed that after either CCTC or DOX treatment, massive cancer cell remission occurred in the tumor tissue (Figure 4b), indicating successful tumor growth inhibition by CCTC. As expected, body weight loss and liver toxicity showed the obvious side effects of chemotherapy (Figure 4c and d), however, CCTC was much more biologically friendly as no body weight loss and no liver toxicity was noted (Figure 4c and d). Both FA and calcium are essential ingredients in human metabolism,^[11] therefore, FA or Ca treatment alone resulted in negligible inhibition and no weight loss (Figure S6). This drug-free feature is a primary advantage of CCTC.

In addition, materials in contact with cancer cells have exhibited great potential for inhibition of tumor metastasis.^[18] Using in vivo and ex vivo organ imaging, fluorescence signals emitted from the tumor in situ and from the lungs were noted (Figure 4e), indicating that the tumor cell had metastasized into the lung site, and visible metastatic nodules were present in the lungs in both the DOX group and other comparisons (Figure 4f; Supporting Information, Figure S7a). Surprisingly, almost no metastases were detected in the CCTC-treatment group (Figure 4e and 4f), indicating CCTC-induced cell encapsulation may suppress tumor metastasis. This suppressed metastatic phenomenon was further confirmed by the measurements of total flux emitted from circulating tumor cells (CTCs) in the blood of mice (Figure 4g), in which the flux was almost undetectable in the CCTC group. In contrast, in the other groups, the detected flux values were always > 450 photons/sec (Figure 4g; Supporting Information, Figure S7b) and accordingly, their mortality rates at day 30 were > 80 % (Figure 4g; Supporting Information, Figure S7c). DOX could effectively inhibit tumor development, but the survival rate was only 20 % owing to the high level of CTC flux (Figure 4g and h), which is consistent with the hypothesis that tumor metastasis is the important lethal factor in solid tumors.^[19] However, at the similar TGI level, the mice survival rate in the CCTC-treatment group was significantly improved to 90 % (Figure 4h) with effectively suppressed metastasis, demonstrating another key advantage of CCTC over chemotherapy.

By using selective calcification as an anticancer tool, CCTC provides a drug-free strategy characterized by efficient tumor inhibition, successful control of metastasis, and improved survival rates, which follows a substitution of sclerosis for tumor disease by using pathological calcification. This proof-of-concept about disease substitution may be developed as an important medical treatment to reduce disease risk.

Acknowledgements

This work is financially supported by the Fundamental Research Funds for the Central Universities of China (ZJU President Program) and the National Natural Science Foundation of China (21571155 and 21201150).

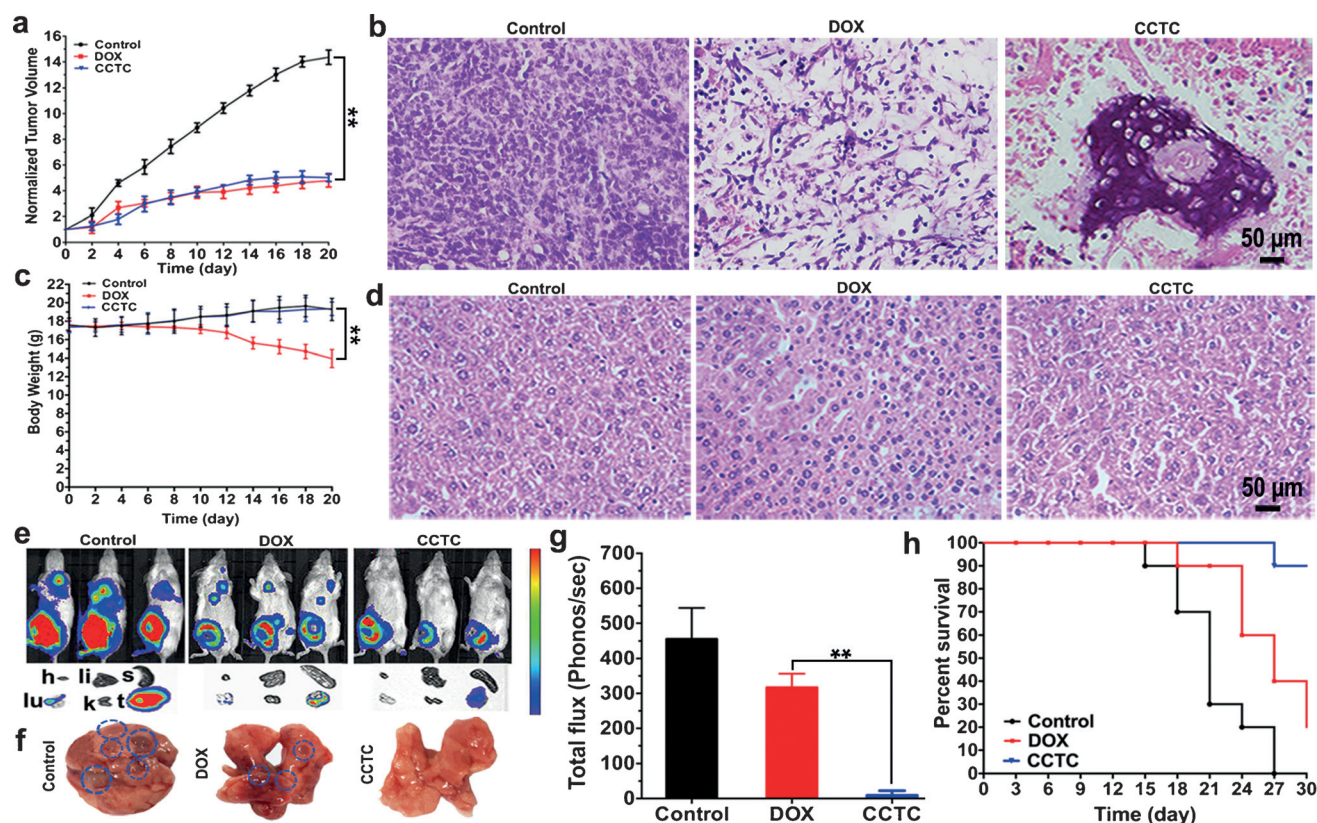


Figure 4. Anticancer therapy by CCTC. a) Normalized tumor growth curves in the control, DOX, and CCTC treatment groups (volume vs. time). b) H&E-stained tumor slices after CCTC and DOX treatments. c) Body weights of mice after the different treatments. d) H&E-stained liver slices after CCTC and DOX treatments. e) Tumor metastasis detection by in vivo imaging (mice) and ex vivo imaging (organs); organs included the heart (h), liver (li), spleen (s), lung (lu), kidney (k), and tumor (t). f) Optical observation of pulmonary metastasis (circles). g) Total flux in mouse blood during DOX and CCTC treatment. Data were collected under similar conditions of TGI. h) Survival rates of the tumor mice after DOX and CCTC treatment ($n = 10$). $^{**}P < 0.01$.

Keywords: bioinorganic chemistry · calcification · cell encapsulation · folate · tumor inhibition

How to cite: *Angew. Chem. Int. Ed.* **2016**, *55*, 5225–5229
Angew. Chem. **2016**, *128*, 5311–5315

- [1] a) L. A. Torre, F. Bray, R. L. Siegel, J. Ferlay, J. Lortet-Tieulent, A. Jemal, *CA Cancer J. Clin.* **2015**, *65*, 87–108; b) R. L. Siegel, K. D. Miller, A. Jemal, *CA Cancer J. Clin.* **2015**, *65*, 5–29.
- [2] a) T. A. Ahles, A. J. Saykin, *Nat. Rev. Cancer* **2007**, *7*, 192–201; b) B. J. Noordman, J. J. B. van Lanschot, *Nat. Rev. Clin. Oncol.* **2015**, *12*, 425–431.
- [3] a) Clinical Outcomes of Surgical Therapy Study, *N. Engl. J. Med.* **2004**, *350*, 2050–2059; b) P. Naredi, M. P. La Quaglia, *Nat. Rev. Clin. Oncol.* **2015**, *12*, 425–431.
- [4] a) T. M. Allen, P. R. Cullis, *Science* **2004**, *303*, 1818–1822; b) D. Peer, J. M. Karp, S. Hong, O. C. Farokhzad, R. Margalit, R. Langer, *Nat. Nanotechnol.* **2007**, *2*, 751–760; c) A. Nel, T. Xia, L. Mädler, N. Li, *Science* **2006**, *311*, 622–627; d) S. Sharifi, S. Behzadi, S. Laurent, M. L. Forrest, P. Stroeve, M. Mahmoudi, *Chem. Soc. Rev.* **2012**, *41*, 2323–2343.
- [5] S. V. Dorozhkin, M. Eppe, *Angew. Chem. Int. Ed.* **2002**, *41*, 3130–3146; *Angew. Chem.* **2002**, *114*, 3260–3277.
- [6] a) L. L. Demer, Y. Tintut, *Circulation* **2008**, *117*, 2938–2948; b) A. P. Sage, Y. Tintut, L. L. Demer, *Nat. Rev. Cardiol.* **2010**, *7*, 528–536.
- [7] a) B. Wang, P. Liu, W. Jiang, H. Pan, X. Xu, R. Tang, *Angew. Chem. Int. Ed.* **2008**, *47*, 3560–3564; *Angew. Chem.* **2008**, *120*, 3616–3620; b) Y. Wei, G. Yin, C. Ma, X. Liao, X. Chen, Z. Huang, Y. Yao, *Med. Hypotheses* **2013**, *81*, 169–171; c) W. Chen, G. C. Wang, R. K. Tang, *Nano Res.* **2014**, *7*, 1404–1428.
- [8] a) J. H. Park, K. Kim, J. Lee, J. Y. Choi, D. Hong, S. H. Yang, F. Caruso, Y. Lee, I. S. Choi, *Angew. Chem. Int. Ed.* **2014**, *53*, 12420–12425; *Angew. Chem.* **2014**, *126*, 12628–12633; b) B. J. Kim, T. Park, H. C. Moon, S. Y. Park, D. Hong, E. H. Ko, J. Y. Kim, J. W. Hong, S. W. Han, Y. G. Kim, I. S. Choi, *Angew. Chem. Int. Ed.* **2014**, *53*, 14443–14446; *Angew. Chem.* **2014**, *126*, 14671–14674; c) W. Li, W. Bing, S. Huang, J. Ren, X. Qu, *Adv. Funct. Mater.* **2015**, *25*, 3775–3784; d) S. H. Yang, J. Choi, L. Palanikumar, E. S. Choi, J. Lee, J. Kim, I. S. Choi, J. H. Ryu, *Chem. Sci.* **2015**, *6*, 4698–4703; e) S. H. Yang, E. H. Ko, Y. H. Jung, I. S. Choi, *Angew. Chem. Int. Ed.* **2011**, *50*, 6115–6118; *Angew. Chem.* **2011**, *123*, 6239–6242; f) W. Xiong, X. Zhao, G. Zhu, C. Shao, Y. Li, W. Ma, X. Xu, R. Tang, *Angew. Chem. Int. Ed.* **2015**, *54*, 11961–11965; *Angew. Chem.* **2015**, *127*, 12129–12133.
- [9] J. Lee, J. Choi, J. H. Park, M. H. Kim, D. Hong, H. Cho, S. H. Yang, I. S. Choi, *Angew. Chem. Int. Ed.* **2014**, *53*, 8056–8059; *Angew. Chem.* **2014**, *126*, 8194–8197.
- [10] a) P. S. Low, W. A. Henne, D. D. Doorneweerd, *Acc. Chem. Res.* **2008**, *41*, 120–129; b) W. He, H. Wang, L. C. Hartmann, J. X. Cheng, P. S. Low, *Proc. Natl. Acad. Sci. USA* **2007**, *104*, 11760–11765; c) B. Wang, P. Liu, Z. Liu, H. Pan, X. Xu, R. Tang, *Biotechnol. Bioeng.* **2014**, *111*, 386–395.

- [11] a) A. Fleming, A. J. Copp, *Science* **1998**, *280*, 2107–2109; b) R. Schneggenburger, E. Neher, *Nature* **2000**, *406*, 889–893.
- [12] Y. Tu, M. Lv, P. Xiu, T. Huynh, M. Zhang, M. Castelli, Z. Liu, Q. Huang, C. Fan, H. Fang, *Nat. Nanotechnol.* **2013**, *8*, 594–601.
- [13] R. S. Jansen, A. Küçükoğlu, T. G. M. F. Gorgels, P. Borst, *Proc. Natl. Acad. Sci. USA* **2013**, *110*, 20206–20211.
- [14] a) D. W. Holdsworth, M. M. Thornton, *Trends Biotechnol.* **2002**, *20*, S34–S39; b) A. Ale, V. Ermolayev, M. H. de Angelis, V. Ntziachristos, *Nat. Methods* **2012**, *9*, 615–620.
- [15] E. Woldt, J. Terrand, M. Mlih, S. Foppolo, Z. El Asmar, M. E. Chollet, E. Ninio, *Nat. Commun.* **2012**, *3*, 1077–1086.
- [16] P. Amarengo, C. Duyckaerts, C. Tzourio, D. Hénin, M. G. Bousser, J. J. Hauw, *N. Engl. J. Med.* **1992**, *326*, 221–225.
- [17] D. S. Kohane, R. Langer, *Chem. Sci.* **2010**, *1*, 441–446.
- [18] R. R. Arvizo, S. Saha, E. Wang, J. D. Robertson, R. Bhattacharya, P. Mukherjee, *Proc. Natl. Acad. Sci. USA* **2013**, *110*, 6700–6705.
- [19] C. L. Chaffer, R. A. Weinberg, *Science* **2011**, *331*, 1559–1564.

Received: February 6, 2016

Published online: March 17, 2016